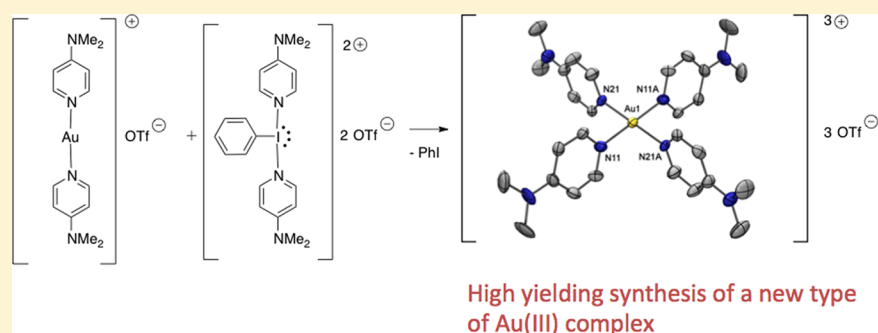


Facile Formation of Homoleptic Au(III) Trications via Simultaneous Oxidation and Ligand Delivery from $[\text{PhI}(\text{pyridine})_2]^{2+}$

Robert Corbo, Thomas P. Pell, Bradley D. Stringer, Conor F. Hogan, David J. D. Wilson, Peter J. Barnard, and Jason L. Dutton*

Department of Chemistry, La Trobe Institute for Molecular Science, La Trobe University, Melbourne, Victoria 3086, Australia

S Supporting Information



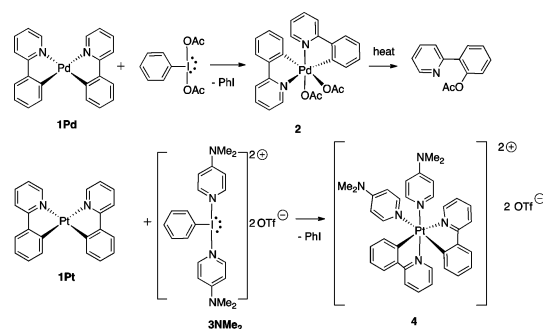
ABSTRACT: We report the first examples of Au(III) tricationic complexes bound only by neutral monodentate ligands, which are a new class of gold reagents. Oxidative addition to the bis-pyridine Au(I) cation, $[\text{Au}(4\text{-DMAP})_2]^+$, using a series of dicationic I(III) oxidants of the general form $[\text{PhI}(\text{L})_2]^{2+}$ (L = pyridine, 4-DMAP, 4-cyanopyridine) allows ready access to homoleptic and pseudo-homoleptic Au(III) complexes $[\text{Au}(4\text{-DMAP})_2(\text{L})_2]^{3+}$. The facile oxidative addition of Au(I) species additionally demonstrates the efficacy of $\text{PhI}(\text{L})_2^{2+}$ reagents as halide-free oxidants for Au(I). Comparisons are made via attempts to oxidize NHC-Au(I)Cl , where introduction of the chloride anion results in complex mixtures via ligand and chloride exchange, demonstrating the advantage of using the pyridine-based homoleptic compounds. The new Au(III) trications show intriguing reactivity with water, yielding dinuclear oxo-bridged and rare terminal Au(III)–OH complexes.

INTRODUCTION

The investigation of high-oxidation state late transition metals, especially palladium, is a topic of current interest in organometallic chemistry.^{1–4} In particular, Sanford has demonstrated the efficacy of I(III) reagents such as PhICl_2 and $\text{PhI}(\text{OAc})_2$ to access Pd(IV) in a variety of stoichiometric and catalytic transformations.^{5–10} In many cases the +4 oxidation state Pd complexes may be isolated and crystallographically characterized, but these remain thermally unstable and reactive toward reductive elimination reactions (e.g., formation of **2** by oxidation of **1Pd** with $\text{PhI}(\text{OAc})_2$ in Scheme 1).^{5,7,9,10} Our group has used the dicationic I(III) reagent 3NMe_2 ^{11,12} to generate Pd(IV) and Pt(IV) complexes such as dicationic complex **4**.¹³ These dicationic I(III) reagents are particularly useful for accessing highly charged metal complexes as they couple oxidation with delivery of neutral ligands to the metal center. Ritter has used such reagents to great effect in a high profile study in which the lability of pyridine ligands from Pd(IV) was used to introduce F^- in a facile way for onward electrophilic fluorination reactions.¹⁴

Recently, oxidation of N-heterocyclic carbene (NHC)-Au(I) complexes to Au(III), using the I(III) oxidizing agent PhICl_2 has been reported (e.g., formation of **6** from **5**).^{15–17} In one report, Blanc and de Frémont described attempts to generate

Scheme 1. Use of I(III) Reagents $\text{PhI}(\text{OAc})_2$ and 3NMe_2 To Generate High Oxidation State Late Metal Complexes **2** and **4**

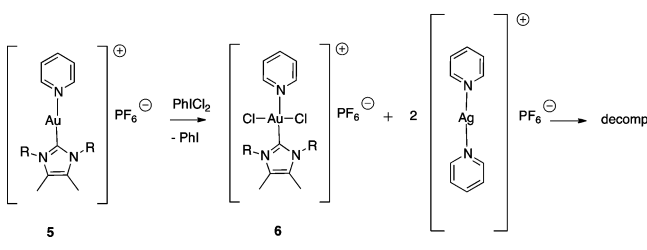


highly charged tricationic Au(III) complexes by replacing two chlorides from the Au(III) compounds with neutral pyridine ligands via silver salt metathesis (Scheme 2), however they were unsuccessful.¹⁵

There are several recent examples of using $\text{PhI}(\text{OAc})_2$ or PhICl_2 as an oxidant in Au(I)/Au(III) catalysis.^{18–23} It has

Received: June 25, 2014

Published: August 12, 2014

Scheme 2. Reported Attempt To Generate NHC/Pyridine Ligated Au(III) Trications by Ag Metathesis from 6


become evident that better results are achieved using $\text{PhI}(\text{OAc})_2$ as the oxidant with Au(I) systems that are completely halide free, in comparison with using a PhICl_2 oxidant or where halides are present on the Au(I) starting material.^{19,22}

Homoleptic Au(III) trications are rare, with the only previously reported examples incorporating chelating ligands. The most well-known example is the bisethylenediamine Au(III) trication,²⁴ which has been investigated for its anticancer properties.²⁵ A handful of examples with macrocyclic N-based ligands^{26,27} or chelating sulfide ligands are also known.²⁸ One example of a tetrakis Au(III) complex with an anionic carbene ligand has also been reported, giving the complex an overall -1 charge.²⁹

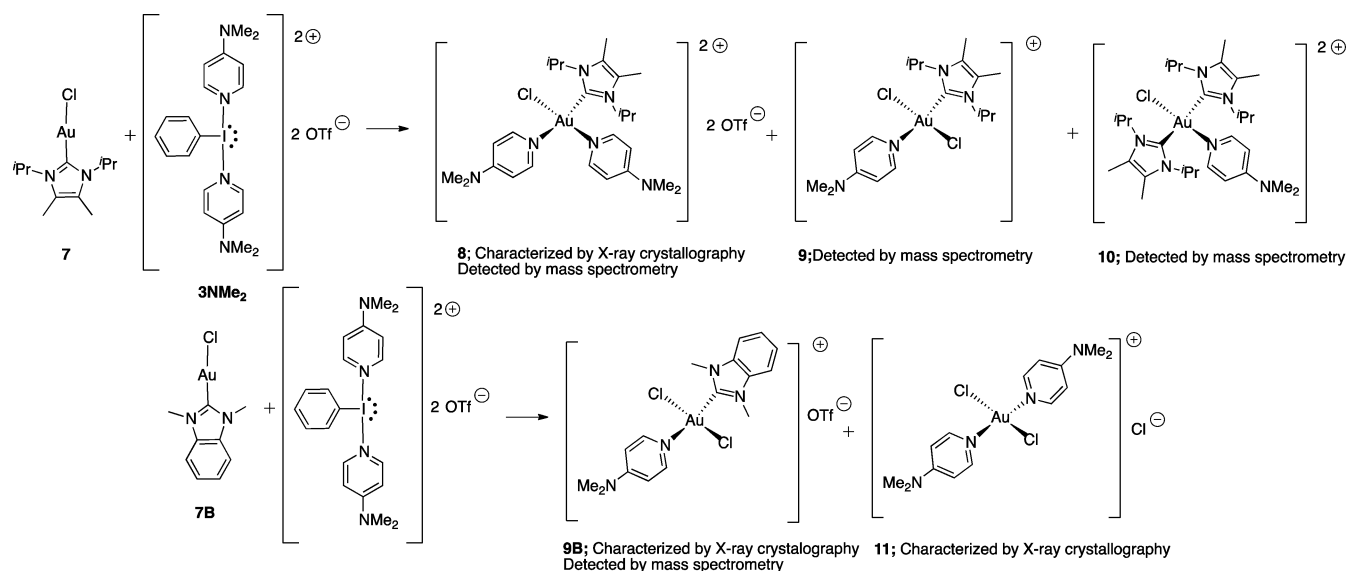
Here we report efforts using I(III) oxidants **3R** ($\text{R} = -\text{NMe}_2, -\text{H}, -\text{CN}$) as a halide-free oxidizing agent leading to the successful synthesis and characterization of homoleptic and pseudo-homoleptic Au(III) centered trications $[\text{Au}(4\text{-DMAP})_2(\text{L})_2]^{3+}$ ($\text{L} = 4\text{-DMAP}, \text{pyridine}, 4\text{-cyanopyridine}$). These represent the first examples of a new class of highly charged gold complexes: trications bound by only monodentate ligands. The reactivity of this new reagent toward water is also described, which yields a facile new route to Au(III)–OH and Au(III)–O–Au(III) species.

RESULTS AND DISCUSSION

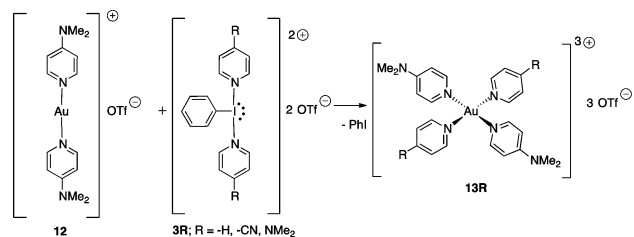
The initial Au(I) starting complex chosen for our study was NHC–Au–Cl complex **7** incorporating Kuhn's NHC.³⁰ Oxidative coupling of NHCs by I(III) reagents is a possible

side reaction, however since the NMR spectroscopic properties of the oxidative coupling product for this NHC are known, its potential formation is easily monitored.¹² The 1:1 stoichiometric reaction between **3NMe**₂ and **7** was carried out in CD_3CN (Scheme 3). The reaction mixture immediately changed from colorless to orange, indicative of a change of oxidation state for Au from +1 to +3. Aliquots were removed for NMR analysis, which revealed a mixture of three NHC and multiple 4-DMAP containing products. Oxidative coupling of the NHC was not observed. Single crystals were grown by vapor diffusion of Et_2O into the NMR sample. X-ray diffraction analysis showed the crystals to be the targeted dicationic product **8** (see Supporting Information for structure), however this compound could not be isolated in a pure form from other cationic Au(III) species. Mass spectrometry analysis of the crude product mixture indicated the other cationic products to be **9** and **10**, apparently arising from ligand exchange and anion scrambling processes. The very similar solubilities of **8–10** precluded the separation of these species. Using a benzimidazolylidene-based NHC (**7B**) in place of **7** also yielded a mixture (Scheme 3), although in this case single crystals of **9B** and **11** could be grown (see Supporting Information). The most abundant signal in the mass spectrum arose from a cation with a formula consistent with **9B**, and as was the case for **7**, no single product could be obtained in a pure form, and the target complex, analogous to **8**, was not observed. It is evident that reactions using NHC–Au–Cl as an Au(I) source results in significant ligand and anion scrambling in the products obtained. Ligand/anion scrambling with other heteroleptic Au(I)/Au(III) systems in the presence of I(III) oxidants has been observed by Nevado and co-workers.^{31,32}

In order to generate the target homoleptic tricationic Au(III) complexes, the Au(I) starting material was changed to the halide-free $[\text{Au}(4\text{-DMAP})_2][\text{OTf}]$ (**12**, Scheme 4) to suppress any possible ligand or anion exchange. Compound **12** is easily synthesized from tHt-AuCl , 4-DMAP, and KOTf . Reaction of **12** with **3NMe**₂ in CH_3CN (Scheme 4) resulted in the immediate production of a deep orange solution. The solvent was removed, and after a short work up a proton NMR spectrum of the powder in CD_3CN gave a set of resonances

Scheme 3. Distribution of Products Observed in Reactions of 7 and 7B with 3NMe₂


Scheme 4. Synthesis of Au(III) Trications 13R



consistent with a single 4-DMAP containing product. Single crystals were grown from a CH₃CN solution of the compound via vapor diffusion of Et₂O, and subsequent X-ray diffraction studies confirmed the compound to be the target compound **13NMe₂** (Figure 1), which is isolated in an 82% yield from the

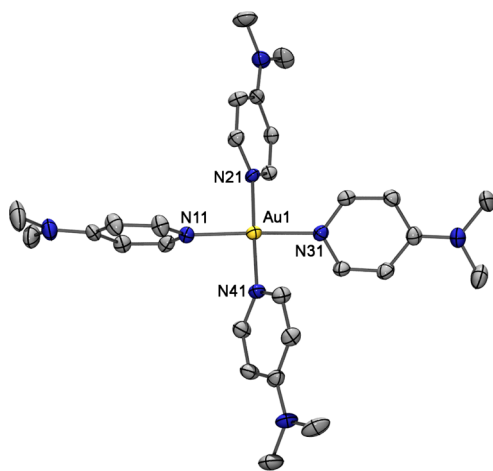


Figure 1. Solid-state structure of the Au(III) trication in **13NMe₂**. Thermal ellipsoids are depicted at 50% probability level. Hydrogen atoms, triflate anions, and acetonitrile solvate are omitted for clarity. Selected bond distances (Å) and angles (deg), with M06-L/def2-TZVP calculated values in square brackets: Au(1)–N(11) 2.021(3) [2.060], Au(1)–N(21) 2.016(3) [2.060], N(11)–Au(1)–N(21) 90.3(1) [90.0], N(11)–Au(1)–N(31) 176.9 [180.0], N(21)–Au(1)–N(41) 178.4(1) [180.0].

reaction. The equivalent reaction of **12** with **3H** and **3CN** yielded the corresponding pseudo-homoleptic compounds **13H** and **13CN**, respectively, also in good yields.

The experimentally determined Au–N bond distances in **13NMe₂** range from 2.008(3) to 2.016(3) Å, which are in close agreement with theoretical results. The 4-DMAP ligands are arranged in the expected square-planar geometry about the Au center. Dicationic homoleptic tetrakis 4-DMAP ligated species are known for Pd, Se, and Te, all of which display a strict *D*_{4h} symmetry in the solid state, which is also the calculated global minimum for **13NMe₂**.^{33–35} In the solid state the symmetry is distorted by rotation of the 4-DMAP ligands. This is likely driven by long contacts with O atoms of the triflate anions (2.862(5) and 3.0826(5) Å) completing a pseudo-octahedral geometry about the Au(III) center in the solid state as well as substantial hydrogen bonding between the triflates and the hydrogen atoms about the pyridine rings in the 4-DMAP ligands. For **13H** the Au–N bond distances are 2.023(4) and 2.030(4) Å (2.077 Å from M06-L/def2-TZVP) for the bond involving pyridine and very slightly shorter at 2.011(4) and 2.017(4) Å (2.061 Å, M06-L/def2-TZVP) for the bond to the

4-DMAP ligands, although the distortion is likely not significant. The solid-state contacts with triflate anions are shorter with two contacts at 2.850(4) and 2.902(5) Å each for the two independent Au atoms in the asymmetric unit, respectively. Finally for **13CN** the Au–N bonds range from 2.004 to 2.026 Å for 4-DMAP and 2.002–2.033 Å for cyanopyridine across two independent trications in the solid-state. While these differences are not statistically significant, the solid-state contacts with the triflate anions are significantly shorter in this derivative ranging from 2.76 to 2.84 Å, overall indicating the gold atom becomes more electron poor moving from 4-DMAP to pyridine to cyanopyridine for the two ligands being modified.

Cyclic voltammetric studies of **13R** show two main irreversible reduction processes (Figure 2), the first corre-

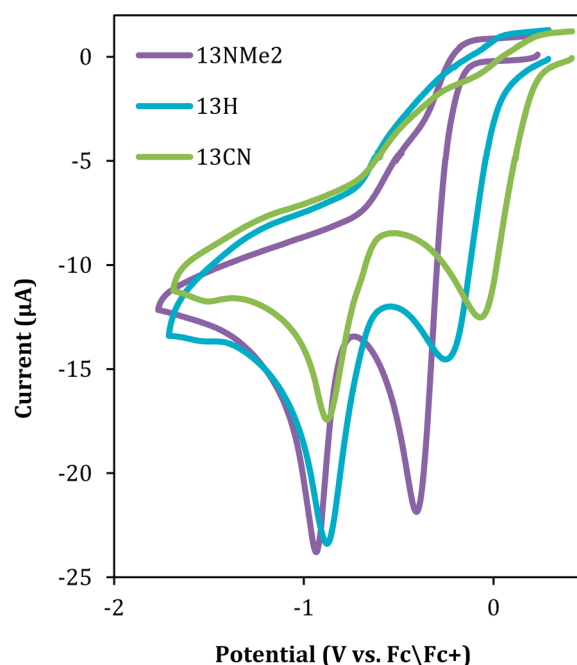


Figure 2. Cyclic voltammetric responses for **13NMe₂**, **13H** and **13CN** using a glassy carbon disk working electrode ($\varnothing = 3$ mm) at a scan rate of 0.1 V s⁻¹. Concentration for each compound was 1 mM, dissolved in acetonitrile containing 0.1 M [Bu₄N][PF₆] as supporting electrolyte. The voltammetric response for **18** is shown in Supporting Information (Figure S24).

sponding to the two-electron reduction of the trication and the second attributable to the further reduction to Au(0). The irreversibility of these peaks is maintained over a broad range of scan rates as shown by Figure S23 in Supporting Information. The reoxidation processes are also visible at more positive potentials. As shown by the data in Table 1, the trications of **13R** are reasonably oxidizing, with potentials for the Au(III) →

Table 1. Electrochemical Properties of **13R** and **18** in Acetonitrile (Conditions as in Figure 2)

	potential vs Fc/Fc ⁺			
	<i>E</i> ^o (ligand)	<i>E</i> _{p,red} (Au ^{I/0})	<i>E</i> _{p,red} (Au ^{III/I})	<i>E</i> _{p,ox}
13NMe₂	–	–0.93	–0.41	0.82
13H	–	–0.87	–0.22	1.28
13CN	–	–0.87	–0.04	1.27
18	–2.52	–0.79	0.21	0.92/1.24

Au(I) process ranging from -0.41 to -0.04 V vs Fc/Fc^+ . The potentials for the reduction of the Au^{3+} species increase in the order $13\text{NMe}_2 < 13\text{H} < 13\text{CN}$, consistent with the decreasing electron donating ability of the ligands. These redox potentials are in the expected range based on previous reports; for example, McArdle and Bossard reported a value of 0.458 V vs SCE (0.069 V vs Fc/Fc^+) for bis[1,2-bis(diphenylphosphino)ethane]Au(I/III).³⁶

The increased favorability of the Au(III)–Au(I) reduction in going from 13NMe_2 to 13CN is consistent with the B3LYP/def2-TZVP calculated HOMO–LUMO gaps, which decrease from 3.03 eV in 13NMe_2 to 2.68 eV in 13H and 2.40 eV in 13CN . The narrowing of the HOMO–LUMO gap is consistent with the observed UV–vis results, where the weak π – σ^* transition responsible for the color of the compounds is red-shifted from 392 nm in 13NMe_2 to 427 and 461 nm in 13H and 13CN , respectively.

The significant alteration in the potential of the first reduction process (~ 400 mV) on replacing the ligands is in contrast with the case for the second one-electron reduction peak, which remains relatively invariant (~ 50 mV). This observation is consistent with a reductive elimination process and suggests that the irreversible nature of the reductions can be traced to the population of the LUMO (Figure 3), which is σ -antibonding with respect to the gold–nitrogen bonds, i.e., reduction essentially furnishes the cationic Au(I) starting material **12**.

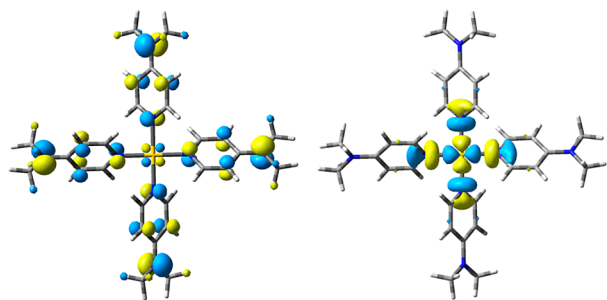


Figure 3. HOMO (left) and LUMO (right) of 13NMe_2 .

Although the reactions must be carried out under anhydrous conditions due to the extreme sensitivity of 3NMe_2 , once the reaction is complete 13NMe_2 is stable in an ambient atmosphere. Compound 13NMe_2 was crystallized from “wet” acetonitrile outside of the glovebox. A lower quality crystal even contained water in the unit cell. Conversely, when attempts at crystallizing 13H were carried out in ambient atmosphere in CH_3CN , the expected structure was not obtained, but rather the X-ray structure that was obtained was that of tetracationic digold compound **14** (Figure 4, Scheme 5). A bridging oxo-unit links together the gold atoms ($\text{Au}–\text{O}$ 1.956 , 1.952 Å), which features an Au–Au contact of 3.336 Å. M06-L/def2-TZVP calculated bond distances are 1.990 and 3.515 Å, respectively.

An acetonitrile solvate is present in a bridging manner to the two Au atoms ($\text{Au}–\text{N}$ 3.232 , 3.345 Å), which is near to the sum of the van der Waals radii for Au and N (3.21 Å).³⁷ Recent work by Alvarez gives a larger value of 3.98 Å for the sum of the van der Waals radii for Au and N.³⁸ Bridging acetonitrile ligands for late metals are quite rare and of current interest.³⁹ While this interaction is likely not retained in solution, it is the first such example in the solid-state for gold.

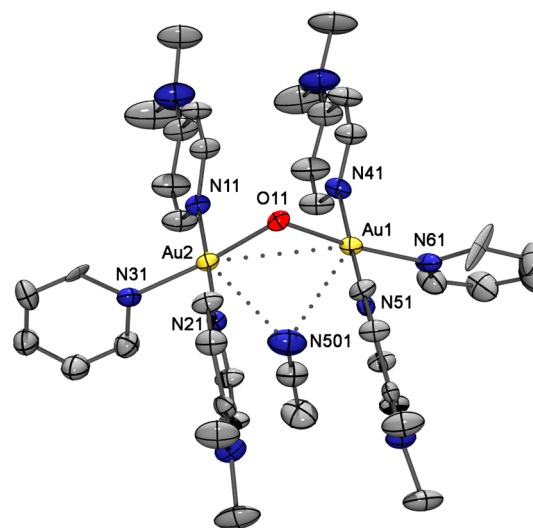
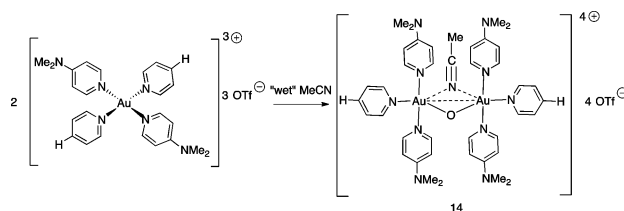


Figure 4. Solid-state structure of the Au(III) tetracation in **14**. Thermal ellipsoids are depicted at 50% probability level. Hydrogen atoms, acetonitrile solvate, and triflate anions are omitted for clarity. Selected bond distances (Å) with M06-L/def2-TZVP calculated values in square brackets: Au(2)–N(11) $2.004(7)$ [2.065], Au(2)–N(31) $2.056(7)$ [2.108], Au(2)–O(11) $1.952(6)$ [1.985], Au(1)–Au(2) $3.3357(8)$ [3.449], Au(1)–N(S01) $3.23(1)$ [3.230], Au(2)–N(S01) $3.35(1)$ [3.357].

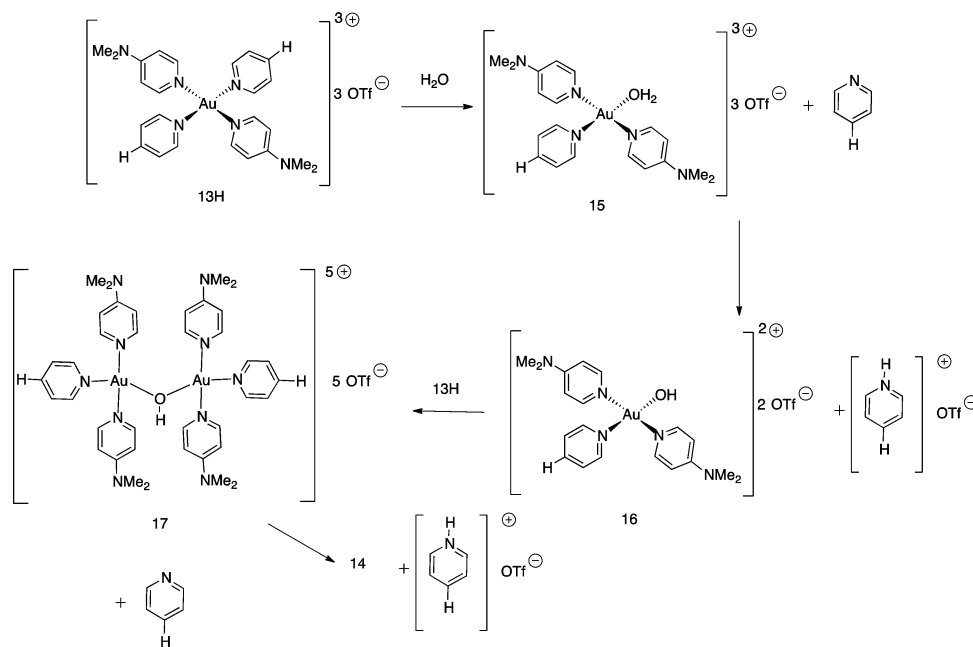
Scheme 5. Synthesis of Au(III) Tetracation **14**



Compound **14** could be synthesized in an intentional manner by simply dissolving 13H in H_2O , stirring for 2 h, followed by a short workup. The interaction of water and oxo species with Au(III) has been a topic of recent interest,⁴⁰ and with **14** containing only monodentate ligands with a single oxo-bridge, it represents a new addition to this family, synthesized directly from water.

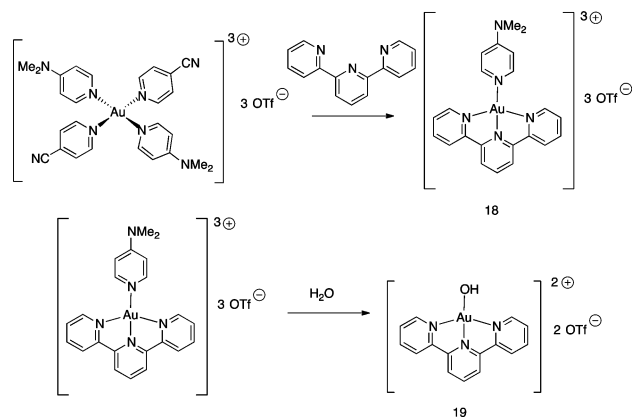
A possible pathway to compound **14** is depicted in Scheme 6. A pyridine ligand is first displaced from 13H by a water molecule giving the water adduct **15**, which is in turn deprotonated by the displaced pyridine giving an Au(III)–OH species (**16**). This species then displaces a pyridine from another molecule of 13H yielding **17**, which is then deprotonated by the second liberated pyridine giving the final product. It is also possible that **14** is generated from a condensation reaction between two molecules of **16** as a similar transformation was observed by Bochmann.⁴⁰ In their study an Au–O–Au compound could be interconverted to two Au–OH moieties via the addition of water, and the reverse reaction to Au–O–Au accomplished by drying the Au–OH compound. However, in our reaction, increasing the water concentration accelerates production of **14**. Monitoring the reaction using ^1H NMR *in situ* carried out in D_2O confirms that the only products are **14** and two equivalents of protonated pyridine relative to **14**, as compared to the ^1H NMR spectrum of a sample independently generated from pyridine and HCl. The reaction

Scheme 6. Proposed Pathway to Compound 14



proceeds to completion in approximately 6 h in D_2O , and no distinct intermediates were observed in the NMR study. To lend support to the Au–OH intermediate **16** being involved in the pathway, a derivative using a multidentate ligand (terpyridine (terpy)) was synthesized. Compounds **13NMe₂** and **13H** do not react with the terpy, but reaction of terpy with **13CN** resulted in a ligand exchange reaction that was completed over the course of 2 days (Scheme 7). Proton

Scheme 7. Synthesis of Compounds 18 and 19



NMR spectra of the resulting deep purple solid indicated that two cyanopyridine and one 4-DMAP ligands were displaced by terpy. Synthesis of compound **18** was confirmed by X-ray crystallography studies on single crystals (Figure 5). Compound **18** has a more favorable Au(III)/Au(I) reduction potential compared to **13CN** (0.21 V vs Fc/Fc^+) as well as a smaller B3LYP/def2-TZVP HOMO–LUMO gap (2.27 eV). A large tail into low-energy visible absorption is responsible for the purple color of the salt ($\lambda = 475$ nm), which could be interpreted as the compound being less stable, and therefore its generation from **13CN** is likely to be entropically driven. The M06-L/def2-TZVP calculated change in entropy for produc-

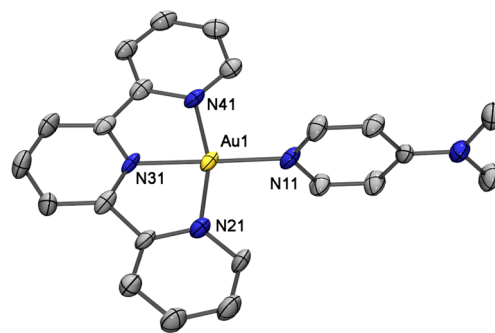


Figure 5. Solid-state structure of the Au trication in compound **18**. Hydrogen atoms, benzene solvate, and triflate anions are omitted for clarity. Selected bond distances (Å) and angles (deg) with M06-L/def2-TZVP calculated values in square brackets: Au(1)–N(11) 1.994(5) [2.067], Au(1)–N(21) 2.015(5) [2.005], Au(1)–N(31) 1.935(5) [2.085], N(11)–Au(1)–N(31) 176.6(2) [177.4], N(21)–Au(1)–N(41) 162.9(2) [159.5], N(21)–Au(1)–N(31) 81.4(2) [79.9].

tion of **18** from **13CN** is substantial at 291 J/mol ($\Delta_r H^\circ = +7$ kJ/mol; $\Delta_r G^\circ = -80$ kJ/mol with acetonitrile solvent).

Exposure of **18** to CH_3CN spiked with a small amount of water resulted in the isolation of compound **19** as confirmed by NMR and X-ray crystallographic studies. This allows for the inference that intermediate **16** is likely involved as an intermediate in the production of **14**, although the specific pathway from **16** to **14** remains speculative. The production of compound **19** is also significant in that very few terminal Au(III)–OH compounds are known, and they are of increasing interest.⁴¹ The dication in **19** has been reported but is one of only two crystallographically characterized terminal Au(III) hydroxides.⁴² The previous synthesis involved activation of an Au–Cl bond with $AgClO_4$ followed by hydroxide. Our generation of this same compound uses only water, which is clearly advantageous. The ease with which this extremely rare type of compound can be synthesized from the pyridine bound

Au trications is hopefully an indication of the potential chemistry to be unlocked with this new family of compounds.

CONCLUSIONS

Homoleptic Au(III) trications are rare, with the only previously reported examples incorporating chelating ligands. Compound **13NMe₂** represents the first homoleptic Au(III) trication bound by monodentate neutral ligands. The pseudo-homoleptic **13H** and **13CN** compounds are also bound only by monodentate ligands, which together with **13NMe₂** represent a new class of Au compound.

Results indicate that the highly charged Au(III) center in these compounds is kinetically active with respect to ligand exchange reactions, which was unproductive in the chloride containing NHC–Au–Cl system but could be exploited in the homoleptic pyridine based systems to access interesting transformations involving water. In particular, this system allows for access to Au(III)–OH species, which is of current major interest. Electrochemical studies demonstrated that the oxidative ability of these tricationic Au(III) compounds could be readily adjusted over a relatively wide range by subtle variation of the ligands, demonstrating the potential for tunability of these systems. The variation of two of the ligands about gold also demonstrated chemical tunability, as **13NMe₂** is stable in water, while **13H** and **18** react distinctively, giving interesting oxo and hydroxyl compounds taking advantage of both the labile and basic nature of the pyridine ligands.

EXPERIMENTAL PROCEDURES

Reaction of 7 with 3NMe₂. A solution of **3NMe₂** (60 mg, 0.08 mmol) in CD₃CN (3 mL) was added dropwise to a stirred suspension of **7** (33 mg, 0.08 mmol) in CD₃CN (3 mL). The reaction mixture was stirred for 10 min resulting in a deep yellow solution. Single crystals of **8** were grown from a concentrated solution of the crude reaction mixture in CH₃CN at –30 °C.

Reaction of 7B with 3NMe₂. A solution of **3NMe₂** (84 mg, 0.11 mmol) in CD₃CN (3 mL) was added dropwise to a stirred suspension of **7B** (41 mg, 0.11 mmol) in CD₃CN (2 mL). The reaction mixture was stirred for 10 min giving a deep yellow solution. Single crystals of **9B** and **11** were grown using vapor diffusion of Et₂O into a CD₃CN solution of the reaction mixture.

Synthesis of 13NMe₂. A solution of **3** (181 mg, 0.242 mmol) in CH₃CN (10 mL) was added dropwise to a solution of **12** (143 mg, 0.242 mmol) in CH₃CN (10 mL) over 1 min. The solution was then stirred for 10 min giving a deep orange solution. The solvent was removed under reduced pressure and the crude solid was recrystallized from CH₂Cl₂/Et₂O yielding **13NMe₂** as a bright orange solid (225 mg, yield: 82%). Melts with decomposition at 168–170 °C. ESI-MS [M]⁺: *m/z* 983.2 [Au(4-DMAP)₄ 2OTf]⁺. ¹H NMR (CD₃CN, ppm): 7.97 (d, 8H, *J* = 7.8 Hz, *o*-H of pyr) 6.71 (d, 8H, *J* = 7.8 Hz, *m*-H of pyr) 3.10 (s, 24H, N(CH₃)₂); ¹³C NMR (CD₃CN, ppm): 156.0, 145.9, 117.3, 109.4, 39.3. ¹⁹F NMR (CD₃CN, ppm): –77.28; UV–vis (CH₃CN): λ_{max} = 288, 392 nm; Elemental analysis (% found (% calcd)) C, 32.51 (32.87); H, 3.57 (3.56); N, 9.78 (9.89).

Synthesis of 13H. A solution of **3H** (190 mg, 0.289 mmol) in CH₃CN (10 mL) was added dropwise to a solution of **12** (170 mg, 0.289 mmol) in CH₃CN (10 mL) over 1 min. The solution was then stirred for 10 min giving a blood red solution. The solvent was removed under reduced pressure, and the resulting residue was recrystallized from DCM/Et₂O yielding **13H** as a deep red solid (302 mg, yield: 90%). M.P. 143–145 °C; ¹H NMR (CD₃CN, ppm): 8.80 (d, 4H, *J* = 6.7 Hz, *o*-H of pyr) 8.36 (t, 2H, *J* = 7.8 Hz, *p*-H of pyr) 8.00 (d, 4H, *o*-H of DMAP) 7.78 (t, 4H, *J* = 6.7 Hz, *m*-H pyr) 6.68 (d, 4H, *J* = 7.8 Hz, *m*-H of 4-DMAP) 3.09 (s, 12H, N(Me)₂); ¹³C NMR (CD₃CN, ppm): 157.0, 150.9, 146.8, 131.1, 111.3; UV–vis (CH₃CN):

λ_{max} = 292, 427 nm. Elemental analysis (% found (% calcd)) C, 31.08 (30.98); H, 3.00 (2.89); N, 8.12 (8.03).

Synthesis of 13CN. A solution of **3CN** (230 mg, 0.324 mmol) in CH₃CN (10 mL) was added dropwise to a solution of **12** (191 mg, 0.324 mmol) in CH₃CN (10 mL) over 1 min. The solution was then stirred for 10 min giving a deep red solution. The solvent was removed under reduced pressure, and the resulting residue was recrystallized from CH₃CN/Et₂O yielding **13CN** as a burnt orange solid (291 mg, yield: 82%). M.P. 188–192 °C; ¹H NMR (CD₃CN, ppm): 8.95 (d, 4H, *J* = 7.0 Hz, *o*-H of 4-cyanopyr) 8.20 (d, 4H, *J* = 7.0 Hz, *m*-H of cyanopyr) 7.93 (d, 4H, *J* = 7.8 Hz, *o*-H of DMAP) 3.12 (s, 12H, N(Me)₂); ¹³C NMR (CD₃CN, ppm): 157.3, 152.0, 146.6, 133.4, 129.4, 114.9, 111.3, 40.5; UV–vis (CH₃CN): λ_{max} = 290, 461 nm. Elemental analysis (% found (% calcd)) C, 31.68 (31.76); H, 2.66 (2.57); N, 10.31 (10.22).

Synthesis of 14. A solution of **13H** (50 mg, 0.0478 mmol) in H₂O (10 mL) was stirred for 2 h at room temperature in the absence of visible light. Solvent was removed under reduced pressure, and resulting yellow residue was recrystallized from CH₃CN/Et₂O yielding **14** as pale yellow solid (20 mg, 50% yield). Melts with decomposition 48–52 °C. ¹H NMR (CD₃CN, ppm): 8.85 (d, 4H, *J* = 6.6 Hz, *o*-H pyr) 8.15 (t, 2H, *J* = 7.0 Hz, *p*-H pyr) 7.92 (d, 8H, *J* = 7.6 Hz, *o*-H 4-DMAP) 7.73 (t, 4H, *J* = 7.0, *m*-H pyr), 6.42 (d, 2H, *J* = 6, *m*-H 4-DMAP), 3.00 (s, 24H, N(Me)₂); ¹³C NMR (CD₃CN, ppm): 156.4, 149.7, 146.5, 144.7, 130.4, 110.0, 40.0.

Synthesis of 18. A solution of terpyridine (40 mg, 0.172 mmol) in CH₃CN (10 mL) was added to a solution of **13H** (188 mg, 0.172 mmol) in CH₃CN (10 mL). The solution was then stirred for 48 h at room temperature. The solvent was removed under reduced pressure, and the resulting residue was recrystallized from CH₃CN/Et₂O yielding **18** as a deep purple solid (179 mg, yield: 76%); decomposition 220 °C; ¹H NMR (CD₃CN, ppm): 8.86 (t, 1H, *J* = 8.3 Hz, terpy) 8.68 (t, 2H, *J* = 8.0 Hz, terpy) 8.61 (m, 4H, terpy) 8.51 (d, 2H, *J* = 5.9 Hz, *o*-H of 4-DMAP), 8.07 (d, 2H, *J* = 6.0 Hz, terpy), 7.97 (m, 2H, terpy), 7.08 (d, 2H, *J* = 5.9 Hz, *m*-H of 4-DMAP), 3.29 (s, 6H, N(Me)₂); ¹³C NMR (CD₃CN, ppm): 158.4, 156.8, 153.8, 151.0, 147.3, 145.2, 131.1, 129.0, 127.3, 111.1, 39.6; UV–vis (CH₃CN): λ_{max} = 293, 475 nm. Elemental analysis (% found (% calcd)) C, 29.95 (30.04); H, 2.26 (2.12); N, 6.93 (7.01).

Synthesis of 19. A solution of **18** (45 mg, 0.045 mmol) in H₂O (10 mL) was stirred for 2 h at room temperature in the absence of visible light. Solvent was removed under reduced pressure. The resulting purple residue was recrystallized from CH₃CN/Et₂O yielding **19** as pale purple solid (30 mg, 90% yield). Spectral and physical data were consistent with literature reports for the same dication (as a [ClO₄][–] salt).⁴²

ASSOCIATED CONTENT

Supporting Information

X-ray data in cif format. Further experimental procedures. NMR spectra for isolated compounds. Mass spectra of the crude reaction mixtures for the reactions in Scheme 3. Computational details and Cartesian coordinates of optimized geometries. This material is available free of charge via the Internet at <http://pubs.acs.org>.

AUTHOR INFORMATION

Corresponding Author

j.dutton@latrobe.edu.au

Notes

The authors declare no competing financial interest.

ACKNOWLEDGMENTS

We thank the La Trobe Institute for Molecular Science for their generous funding of this work. We thank the Victorian Partnership for Advanced Computing (VPAC), the National Computational Infrastructure National Facility (NCI-NF) and

La Trobe University for computing resources. This work was partially funded by an ARC DECRA (J.L.D.; DE130100186).

REFERENCES

- (1) Hickman, A. J.; Sanford, M. S. *Nature* **2012**, *484*, 177.
- (2) Lyons, T. W.; Sanford, M. S. *Chem. Rev.* **2010**, *110*, 1147.
- (3) Neufeldt, S. R.; Sanford, M. S. *Acc. Chem. Res.* **2012**, *45*, 936.
- (4) Deprez, N. R.; Sanford, M. S. *Inorg. Chem.* **2007**, *46*, 1924.
- (5) Racowski, J. M.; Dick, A. R.; Sanford, M. S. *J. Am. Chem. Soc.* **2009**, *131*, 10974.
- (6) Racowski, J. M.; Ball, N. D.; Sanford, M. S. *J. Am. Chem. Soc.* **2011**, *133*, 18022.
- (7) Whitfield, S. R.; Sanford, M. S. *J. Am. Chem. Soc.* **2007**, *129*, 15142.
- (8) Dick, A. R.; Hull, K. L.; Sanford, M. S. *J. Am. Chem. Soc.* **2004**, *126*, 2300.
- (9) Arnold, P. L.; Sanford, M. S.; Pearson, S. M. *J. Am. Chem. Soc.* **2009**, *131*, 13912.
- (10) Dick, A. R.; Kampf, J. W.; Sanford, M. S. *J. Am. Chem. Soc.* **2005**, *127*, 12790.
- (11) Weiss, R.; Seubert, J. *Angew. Chem., Int. Ed.* **1994**, *33*, 891.
- (12) Pell, T. P.; Couchman, S. A.; Ibrahim, S.; Wilson, D. J. D.; Smith, B. J.; Barnard, P. J.; Dutton, J. L. *Inorg. Chem.* **2012**, *51*, 13034.
- (13) Corbo, R.; Georgiou, D. C.; Wilson, D. J. D.; Dutton, J. L. *Inorg. Chem.* **2014**, *53*, 1690.
- (14) Lee, E.; Kamlet, A. S.; Powers, D. C.; Neumann, C. N.; Boursalian, G. B.; Furuya, T.; Choi, D. C.; Hooker, J. M.; Ritter, T. *Science* **2011**, *334*, 639.
- (15) Orbisaglia, S.; Jacques, B.; Braunstein, P.; Hueber, D.; Pale, P.; Blanc, A.; Frémont, P. *Organometallics* **2013**, *32*, 4153.
- (16) Huynh, H. V.; Guo, S.; Wu, W. *Organometallics* **2013**, *32*, 4591.
- (17) Ghidui, M. J.; Pistner, A. J.; Yap, G. P. A.; Lutterman, D. A.; Rosenthal, J. *Organometallics* **2013**, *32*, 5026.
- (18) Zhang, D.; Dai, L.; Shi, M. *Eur. J. Org. Chem.* **2010**, 5454.
- (19) Iglesias, A.; Muniz, K. *Chem.—Eur. J.* **2009**, *15*, 10563.
- (20) Kar, A.; Mangu, N.; M, K. H.; Beller, M.; Tse, M. K. *Chem. Commun.* **2008**, 386.
- (21) de Haro, T.; Nevado, C. *J. Am. Chem. Soc.* **2010**, *132*, 1512.
- (22) Li, Z.; Ding, X.; He, C. *J. Org. Chem.* **2006**, *71*, 5876.
- (23) Pradal, A.; Toullec, P. Y.; Michelet, V. *Org. Lett.* **2011**, *13*, 6086.
- (24) Block, B. P.; Bailar, J. C. *J. Am. Chem. Soc.* **1951**, *73*, 4722.
- (25) Messori, L.; Abbate, F.; Marcon, G.; Orioli, P.; Fontani, M.; Mini, E.; Mazzei, T.; Carotti, S.; O'Connell, T.; Zanello, P. *J. Med. Chem.* **2000**, *43*, 3541.
- (26) Kimura, E.; Kurogi, Y.; Takahashi, T. *Inorg. Chem.* **1991**, *30*, 4117.
- (27) Kimura, E.; Kurogi, Y.; Koike, T.; Shionoya, M.; Itaka, Y. *J. Coord. Chem.* **1993**, *28*, 33.
- (28) Huang, D.; Zhang, X.; McInnes, E. J. L.; McMaster, J.; Blake, A. J.; Davies, E. S.; Wolowska, J.; Wilson, C.; Schroder, M. *Inorg. Chem.* **2008**, *47*, 9919.
- (29) Wehlan, M.; Thiel, R.; Fuchs, J.; Beck, W.; Fehlhammer, W. P. J. *Organomet. Chem.* **2000**, *613*, 159.
- (30) Kuhn, N.; Kratz, T. *Synthesis* **1993**, 561.
- (31) Hofer, M.; Nevado, C. *Eur. J. Inorg. Chem.* **2012**, 1338.
- (32) Hofer, M.; Nevado, C. *Tetrahedron* **2013**, *69*, 5751.
- (33) Dutton, J. L.; Tuononen, H. M.; Ragona, P. J. *Angew. Chem., Int. Ed.* **2009**, *48*, 4409.
- (34) Dutton, J. L.; Battista, T. L.; Sgro, M. J.; Ragona, P. J. *Chem. Commun.* **2010**, *46*, 1041.
- (35) Flanagan, K. A.; Sullivan, J. A.; H, B.-M. *Langmuir* **2007**, *23*, 12508.
- (36) McArdle, J. V.; Bossard, G. E. J. *Chem. Soc., Dalton Trans.* **1990**, 2219.
- (37) Pauling, L. *The Nature of the Chemical Bond*; Cornell University Press: Ithaca, NY, 1960.
- (38) Alvarez, S. *Dalton Trans.* **2013**, *42*, 8617.
- (39) Davenport, T. C.; Tilley, T. D. *Angew. Chem., Int. Ed.* **2011**, *50*, 12205.
- (40) Rosca, D.; Wright, J. A.; Hughes, D. L.; Bochmann, M. *Nat. Commun.* **2013**, *4*, 2167.
- (41) Rosca, D.; Smith, D. A.; Bochmann, M. *Chem. Commun.* **2012**, *48*, 7247.
- (42) Pitteri, B.; Marangoni, G.; Visentin, F.; Bobbo, T.; Bertolasi, V.; Gilli, P. *J. Chem. Soc., Dalton Trans.* **1999**, 677.